Supporting Information

Biomimetic Synthesis of 2D Ultra-small Copper Sulfide Nanoflake Based on Reconfiguration of Keratin Secondary Structure for Caner Theranostics in NIR-II

Guangzong Min,‡ [a] Fengqiu Hong,‡ [b] Chenyang Shi, [a] Qingliang Zhao, [b] Naibo Lin, [a]* and Xiang-Yang Liu [c]**

a. College of Materials, Xiamen University, 422 Siming Nan Road, Xiamen 361005, China
b. State Key Laboratory of Molecular Vaccinology and Molecular Diagnostics, Center for Molecular Imaging and Translational Medicine, School of Public Health, Xiamen University, Xiamen 361102, China Shenzhen Research Institute of Xiamen University, Shenzhen 518063, China.
c. College of Ocean and Earth Sciences, State Key Laboratory of Marine Environmental Science (MEL), Xiamen University, Xiamen 361005, China

*Authors to whom correspondence should be addressed. E-mail address: zhaoql@xmu.edu.cn (Qingliang Zhao), linnaibo@xmu.edu.cn (Naibo Lin), and liuxy@xmu.edu.com (Xiang-Yang Liu)

KEYWORDS α-keratin, secondary structure, CuS nanoflake, second near infrared, cancer theranostics

Materials. All reagents used are analytical grade without additional purification. All solutions were prepared in Milli-Q water (18 $M\Omega \cdot cm^{-1}$). Wool fibers were kindly supplied by Tongxiang Dushi Woolen Material Co., BSA powder, methyl thiazolyl tetrazolium (MTT) and copper chloride dihydrate ($CuCl_2 \cdot 2H_2O$) were provided by Aladdin Industrial Corporation. Calcein acetoxymethyl ester (Calcein AM), propidium iodide (PI) were obtained from Sigma Aldrich (Shanghai) Trading Co. Sodium dodecylsulfate (SDS), sodium sulfide nonahydrate ($Na_2S \cdot 9H_2O$), urea, and sodium hydroxide (NaOH) were purchased from Xilong Chemical Industry.

Instruments. The morphology and crystal structure of the CuS NFs were characterized by a JEM-2100F (JEOL, Japan) field emission high-resolution transmission electron microscope (HRTEM) with an accelerating voltage of 200 kV. Energy-dispersive X-ray (EDS) elemental mapping images were obtained by a Talos F200s HRTEM (FEI, America). The CuS nanoflakes (NFs) in powder were characterized with X-ray diffraction (XRD, Multimode 8, Bruker, USA). Absorption spectra were recorded on a UV−Vis-NIR spectrophotometer (LAMBDA 750, PerkinElmer, France). X-ray photoelectron spectroscopy (XPS, Quantum 2000, PHI, USA) was performed to characterize the inner element chemical state. Fourier transform infrared (FTIR) spectra (Thermo Fisher, USA) and circular dichroism (CD) spectra (Applied Photophysics Limited, Britain) was applied to analyze the secondary structures of the WK@CuS NFs in powder and solution, respectively. The hydrodynamic size was measured using a dynamic light scattering instrument (Mastersizer2000, Malvern, Britain). Photoacoustic (PA) mapping was performed using PA imaging system LAZR-X Vero system (VisualSonics, America).

Preparation of Regenerated WK Solution. WK aqueous solution was prepared from the pretreated wool fiber following a pervious procedure.[1] Briefly, pretreated wool fibers were dissolved in 0.1 L aqueous solution, containing 4 M urea, 0.1 M sodium, and 0.02 M SDS and were heated to 50°C for 12 h. Then, the mixed solution was

dialyzed against distilled water using dialysis tape (SolarBio, molecular cut-off of approximately 10000 Da) for 3 days.

Preparation of WK@CuS NFs. For the synthesis of CuS NFs, an aqueous $CuCl_2 \cdot 2H_2O$ (5 mL, 30 mM) was slowly added into prepared WK solution (10 mL, 20 mg mL^{-1}) under vigorous stirring to bind Cu^{2+} to the WK molecules sufficiently. After 5 min, $Na_2S \cdot 9H_2O$ (5 mL, 30 mM) slowly was added into the mixed solution to introduce more S atom. After 10 min, NaOH (1.0 M) was used to adjust the solutions pH to 12, and the mixture was allowed to react at 90°C under vigorous stirring. During the reaction process, 1 mL of the mixture was taken out and the UV-Vis absorbance of the mixture after be placed into 90°C reaction was detected at different time points. Finally, the mixture was further dialyzed against DI water for 24 h to remove excess precursors. The mixture was freeze-dried and collected for later usage.

Photothermal Effect and Photostability. To evaluate the photothermal effects of CuS NFs, CuS NFs solutions were irradiated at various concentrations of 0, 0.125, 0.25, 0.5, 1, and 2 mg·mL^{-1} under a 1064 nm laser (1 W·cm^{-2}, 10 min), and the temperature was measured *via* an infrared thermal imaging instrument (FLIR, Ax5, America). To evaluate the photostability, a solution of CuS NFs (2 mg·mL^{-1}) in quartz cuvette was irradiated using 1064 nm laser (1 W·cm^{-2}) for 5 min (LASER ON), followed by natural cooling to room temperature without irradiation (LASER OFF). Subsequently, the additional four LASER ON/OFF cycles were further repeated for the photostability. To evaluate the photothermal conversion efficiency, 0.2 mL aqueous dispersion (2 mg·mL^{-1}) were irradiated under a 1064 nm laser with a power density of 1 W·cm^{-2}. When the temperature reached a steady temperature, the irradiation was quit for cooling down to room temperature. The temperature was monitored *via* the infrared thermal imaging instrument.

Photothermal Conversion Efficiency. To evaluate the photothermal conversion efficiency, the temperature change of 200 μL mixed solution was recorded under

continuous irradiation of 1064 nm laser with a power density of 1 W cm^{-2}. The solution was first heated to a steady-state temperature and then cooled to room temperature. The photothermal conversion efficiency, η, was calculated using following equations.[2]

$$\theta = \frac{T - T_{surr}}{T_{max} - T_{surr}} \quad (1)$$

$$t = -\tau_s ln\theta \quad (2)$$

$$hS = \frac{m_{H_2O}C_{H_2O} + m_{quartz}C_{quartz}}{\tau_s} \quad (3)$$

$$Q_{Dis} = hS(T(H_2O)_{max} - T_{surr}) \quad (4)$$

$$\eta = \frac{hS(T_{max} - T_{surr}) - Q_{Dis}}{I(1 - 10^{-A})} \quad (5)$$

Where h (mW cm^{-2} $°C^{-1}$) is the heat transfer coefficient, S (m^2) is surface area of the container. m (H_2O) and C (H_2O) are the mass (200 mg) and heat capacity (4.2 J (g °C)$^{-1}$), respectively; m (quartz) and C (quartz) are the mass (2.65 g) and heat capacity (0.839 J (g °C) $^{-1}$). T_{max} (°C) is equilibrium temperature for WK@CuS NPs solution and water, which is 65.1°C. T_{surr} (°C) is environment temperature, which is 25.73°C. I is power density (1 W cm^{-2}) of laser, A is the absorbance of WK@CuS NFs at 1064 nm (A_{1064}=1.682). τ_s is the sample system time constant, which can be determined by applying the linear time data from the cooling period *vs* –lnθ (τ_s = 113.1). The photothermal conversion efficiency of WK@CuS NFs can be determined to be 32.9%.

Cell Culture. 4T1 cells and L-O2 cells (human normal hepatocytes) were cultured in Dulbecco's modified eagle medium (DMEM) with high glucose supplemented with 10% fetal bovine serum, 100 U mL^{-1} penicillin and 100 mg mL^{-1} streptomycin. Cells were cultured in a 15 mm diameter cell culture dish in an incubator at 37°C and 5% CO_2.

Toxicity Evaluation of WK@CuS NFs for normal cell. Logarithmic growth phase

cells were collected, adjusted to the appropriate concentration, and added into sterile 96-well plates with a total volume of 200 μL per well. The inoculated cell density was about 2×10^4 cells/well. Finally, L-O2 cells were incubated with WK@CuS NFs at the various concentration of 0, 0.05, 0.1, 0.2, 0.3, and 0.4 $mg \cdot mL^{-1}$ for 24 h incubation, and then the cells were washed with PBS for the cell toxicity evaluation.

In Vitro PTT of WK@CuS NFs. 4T1 cells were incubated with CuS NFs solution at the different concentrations of 0.125, 0.25, 0.5, 1, and 2 $mg \cdot mL^{-1}$ for 4 h incubation, and then the cells were washed with PBS, followed by a 5 min irradiation (1064 nm, 1 $W \cdot cm^{-2}$). After another 3 h incubation, a live/dead staining kit was used to differentiate the living cells and dead cells on a fluorescence microscope.

In Vivo PTT of WK@CuS NFs. 4T1 tumor-bearing mice were randomly divided into four groups: (1) laser irradiation; (2) PBS + laser (the same volume with CuS NFs); (3) CuS NFs; (4) CuS NFs + laser. For in vivo photothermal therapy and imaging, when the tumor size reached ~50 mm^3, the tumor-bearing mice were intravenous injected with 200 μL 2 mg mL^{-1} of WK@CuS NFs solution. After 24 h, thermal images were gained by an infrared thermal imaging camera when the tumors were irradiated by 1064 nm (1 $W \cdot cm^{-2}$) for 10 min. After different treatments, the tumor volume and body weight of each group was measured every two days. On the second day of treatment, any mice from each group were measured and related tumor tissues were collected for hematoxylin and eosin (H&E) staining.

Mice were obtained from center of experimental animals, Xiamen University, China. All animal experiments were performed in compliance with the approval of the Institutional Animal Care and Use Committee, and the approval number of XMULAC20190024.

PA Imaging. To evaluate the PA performance of WK@CuS NFs in Vitro, WK@CuS NFs solutions were irradiated at various concentrations of 0, 0.125, 0.25, 0.5, 1, and 2 $mg \cdot mL^{-1}$ by photoacoustic imaging system under a 1200 nm laser. For the in vivo PA

imaging, WK@CuS NFs (2.0 mg mL^{-1}, 200 μL) solution were intravenously injected into a mouse bearing 4T1 tumor. Then, the PA imaging was performed at pre-injection, and 12 h, 24 h, 36 h, 60 h and 120 h post-injection.

In vivo biosafety of WK@CuS NFs. Mice of a similar body weight and age were randomly divided into two groups (n = 6): (1) blank control (treated with PBS); (2) mice injected with WK@CuS NFs. At 14 days post- intravenous injection of WK@CuS NF. In addition, the main organs of mice in the different treatment groups were collected to prepare their paraffin sections (CM1950, Lecia), which were then stained using H&E.

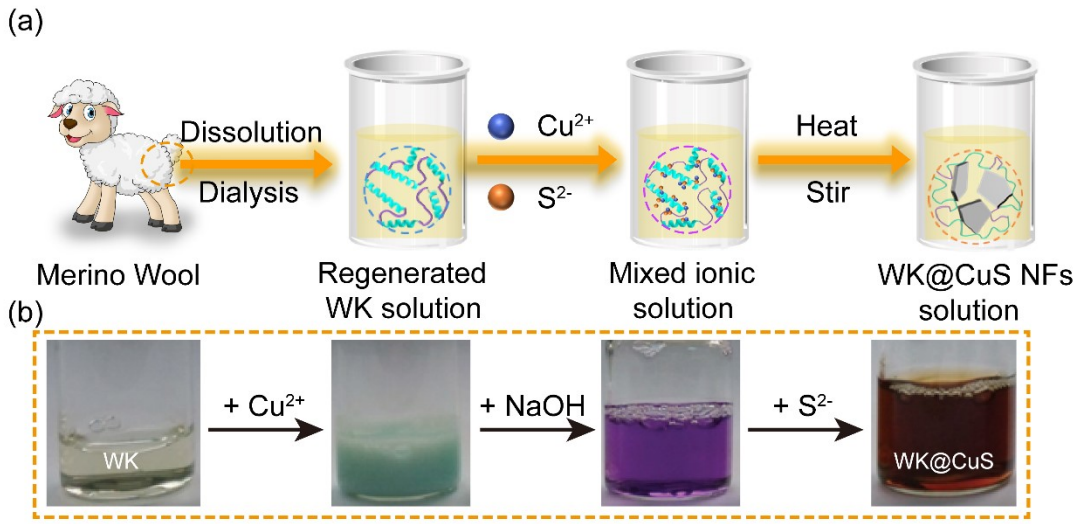

Figure S1. (a) Schematic diagram of wool keratin extraction and synthesis of CuS NF solution. (b) Photographs of synthetic process of WK@CuS NFs.

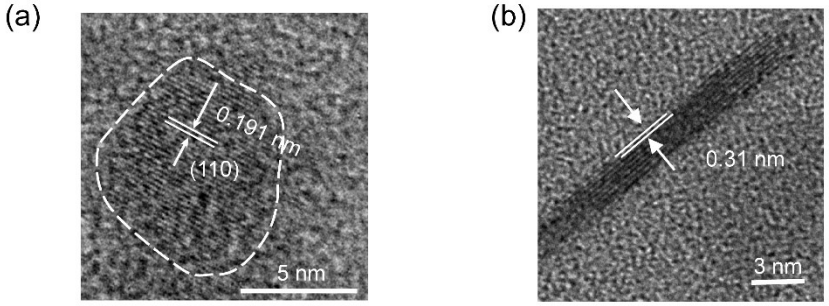

Figure S2. (a) HRTEM image of CuS NFs. (b) vertical direction image of CuS NFs.

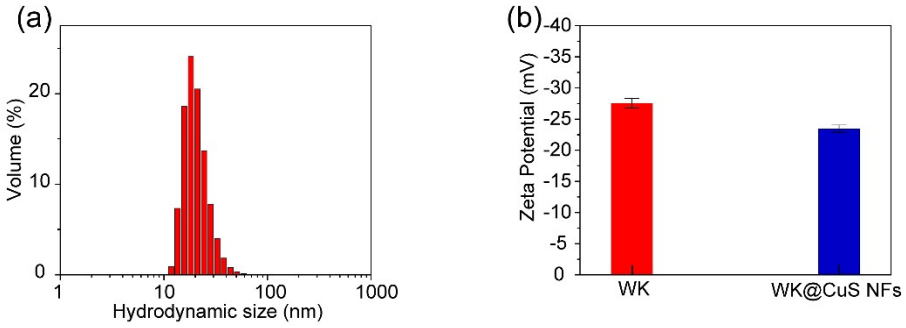

Figure S3. (a) Hydrodynamic size of WK@CuS NFs aqueous solution. (b) Zeta potential of WK and of WK@CuS NFs aqueous solution.

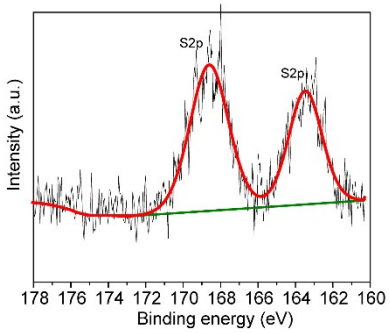

Figure S4. XPS of S element of WK@CuS NFs

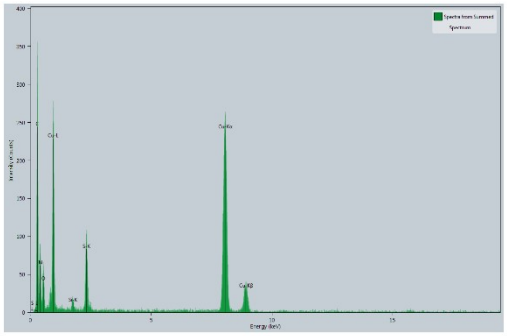

Figure S5. EDS of WK@CuS NFs.

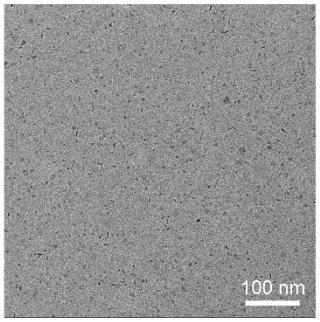

Figure S6. TEM image of BSA@CuS nanoparticle.

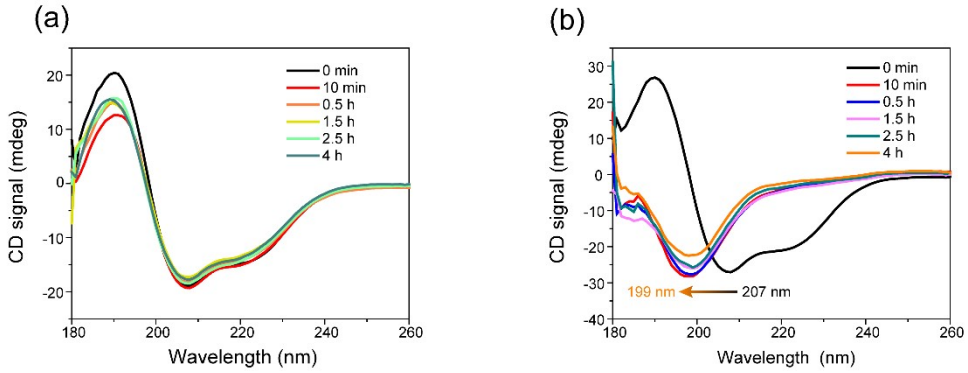

Figure S7. (a) CD signal spectra of the pure wool solution at various reaction time (0 min, 10 min, 0.5 h, 1.5 h, 2.5 h, 4 h) at 90℃, pH=12. (b) CD signal spectra of the mixed solution with Cu^{2+} and WK at various reaction time (0 min, 10 min, 0.5 h, 1.5 h, 2.5 h, 4 h) at 90℃, pH=12.

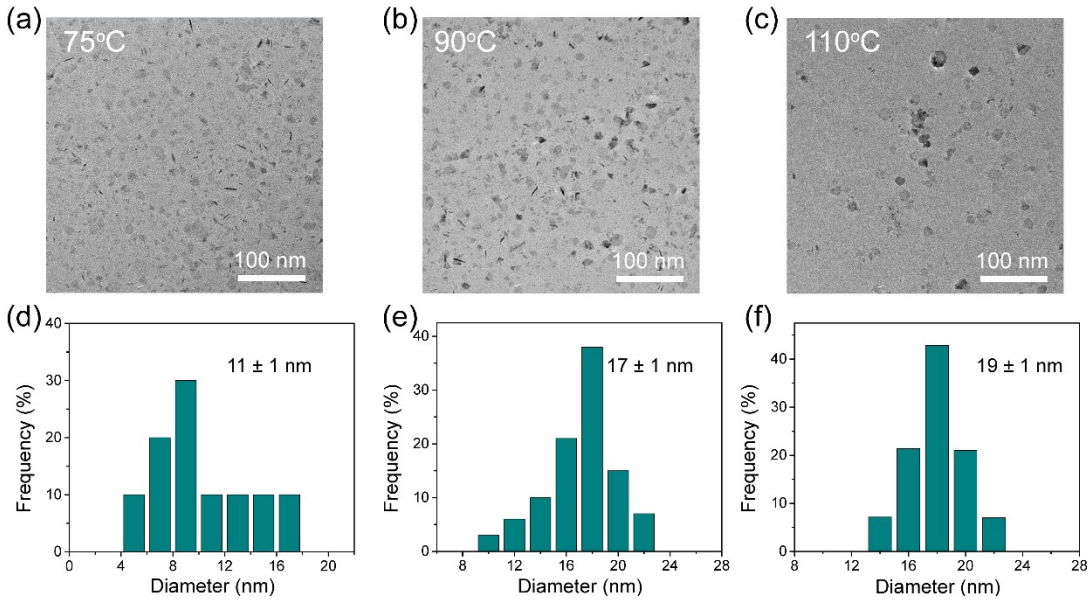

Figure S8. TEM image of WK@CuS NFs prepared with different temperature: (a) 75℃, (b) 90℃, (c) 110℃. Size distribution profiles of CuS NPs prepared with different temperature: (d) 75℃, (e) 90℃, (f) 110℃.

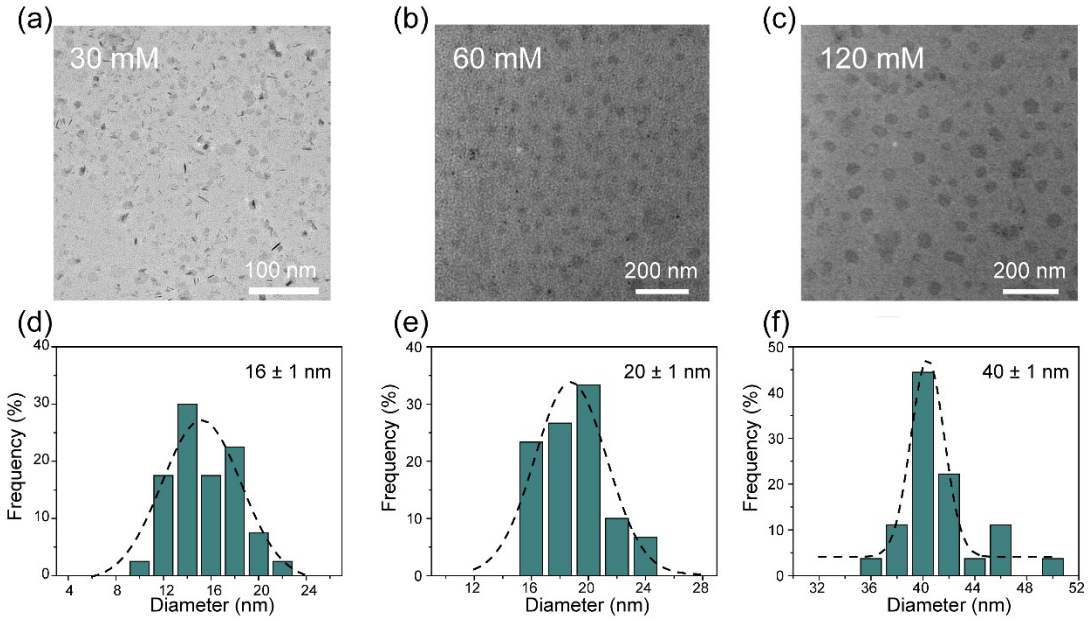

Figure S9. TEM image of WK@CuS NFs prepared with different concentrations of Cu^{2+}: (a) 30 mM, (b) 60 mM, (d) 120 mM. Size distribution profile of CuS NPs prepared with different concentrations of Cu^{2+}: (d) 30 mM, (e) 60 mM, (f) 120 mM.

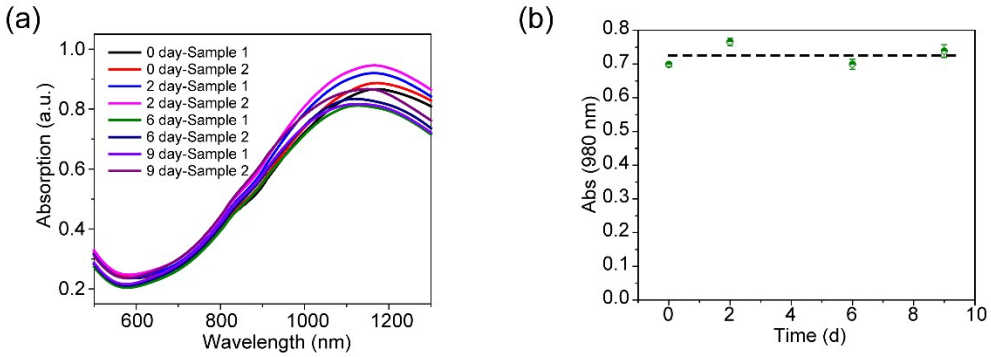

Figure S10. (a) UV-Vis-NIR absorption spectrum with various storage time (0, 2, 6, 9 day, and two samples for each period) at room temperature. (b) Absorption intensity at 980 nm with various storage time (0, 2, 6, 9 day) at room temperature.

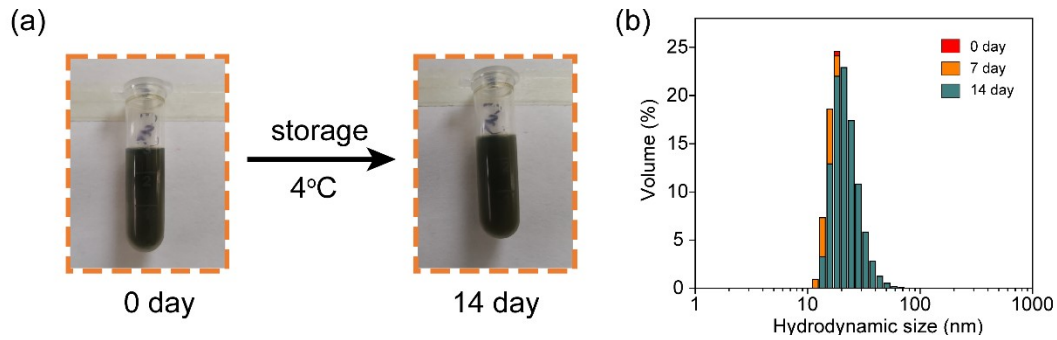

Figure S11. (a) Photographs of WK@CuS NFs solutions. (b) Hydrodynamic size of WK@CuS NF aqueous solution with various storage time (0, 7, 14 day).

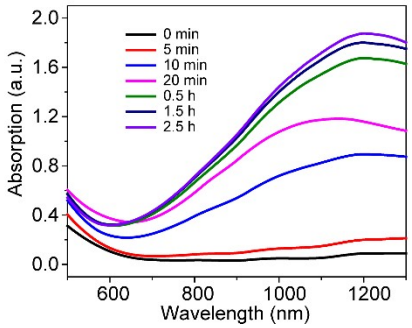

Figure S12. UV-Vis-NIR absorption spectra of WK@CuS NFs with various reaction time.

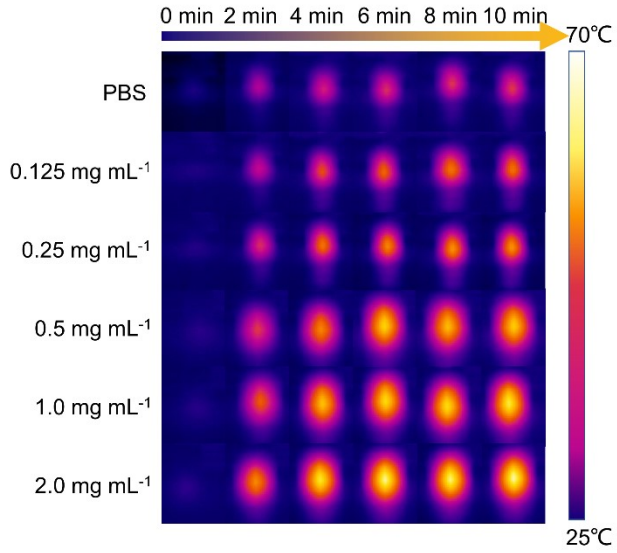

Figure S13. Infrared thermal images of PBS and different concentration of WK@CuS NFs (1064 nm, 1 W/cm^2, 10min).

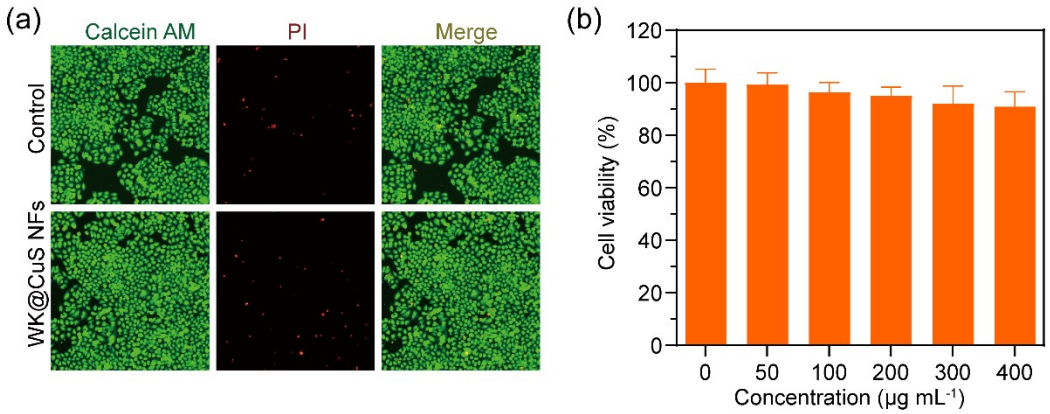

Figure S14. The biocompatibility of the created materials towards normal human cells (L–O2). (a) CLSM images stained with calcein-AM and PI. (b) Relative viabilities incubated with CuS NFs at different concentrations.

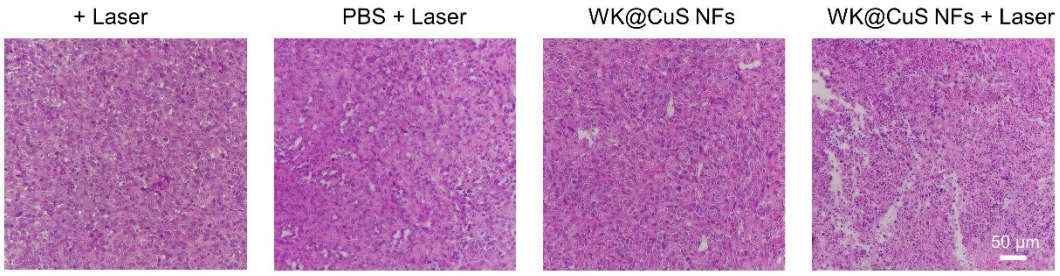

Figure S15. H&E-stained tumor tissues after different treatments.

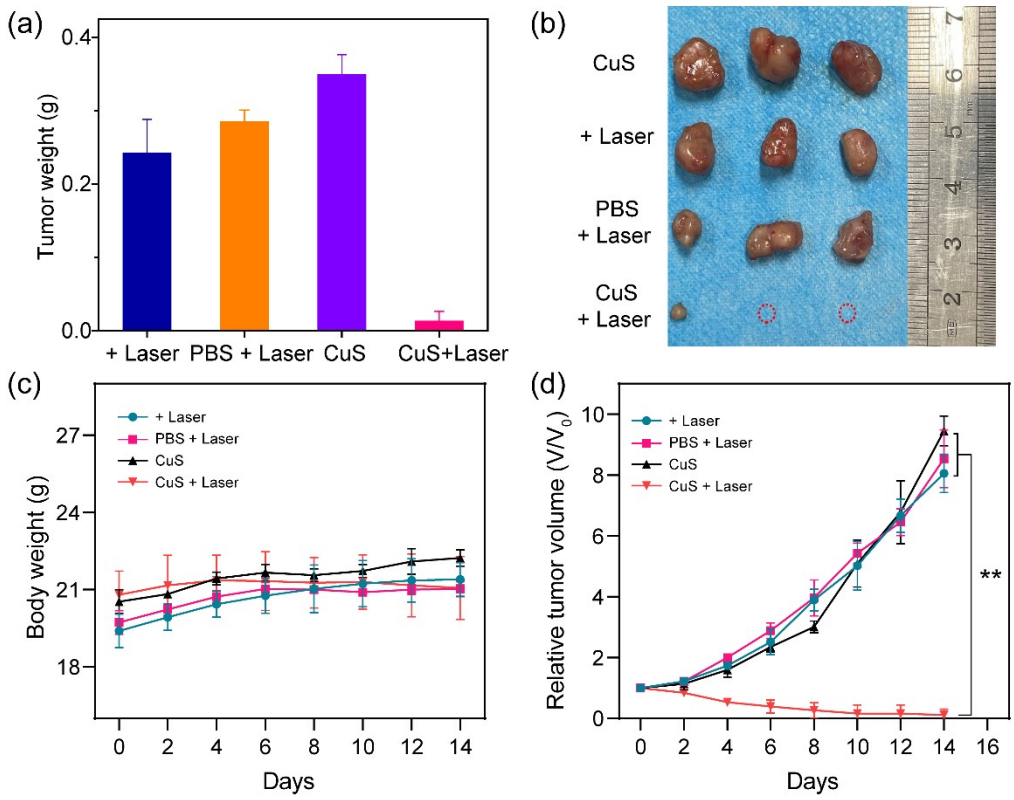

Figure S16. (a) (b) The weight and optical image of tumor after 2 weeks of treatment, (c) mouse body weight curves and (d) tumor growth curves during treatment.

1. C. Shi, Y. Xing, A. Patil, Z. Meng, R. Yu, N. Lin, W. Qiu, F. Hu and X. Y. Liu, *ACS Appl Mater Interfaces*, 2019, **11**, 30125-30136.
2. W. Zhen, Y. Liu, L. Lin, J. Bai, X. Jia, H. Tian and X. Jiang, *Angew. Chem. Int. Ed. Engl.*, 2018, **57**, 10309-10313.